AIP | Journal of Applied Physics

Nano-scale NiSi and n-type silicon based Schottky barrier diode as a near infra-red detector for room temperature operation

S. Roy, K. Midya, S. P. Duttagupta, and D. Ramakrishnan

Citation: Journal of Applied Physics **116**, 124507 (2014); doi: 10.1063/1.4896365
View online: http://dx.doi.org/10.1063/1.4896365
View Table of Contents: http://scitation.aip.org/content/aip/journal/jap/116/12?ver=pdfcov
Published by the AIP Publishing

Articles you may be interested in

Nano-Schottky barrier diodes based on Sb-doped ZnS nanoribbons with controlled p-type conductivity
Appl. Phys. Lett. **98**, 123117 (2011); 10.1063/1.3569590

Ni-catalyzed growth of silicon wire arrays for a Schottky diode
Appl. Phys. Lett. **97**, 042103 (2010); 10.1063/1.3467839

Low-cost and high-gain silicide Schottky-barrier collector phototransistor integrated on Si waveguide for infrared detection
Appl. Phys. Lett. **93**, 071108 (2008); 10.1063/1.2970996

Near-infrared waveguide-based nickel silicide Schottky-barrier photodetector for optical communications
Appl. Phys. Lett. **92**, 081103 (2008); 10.1063/1.2885089

High barrier iridium silicide Schottky contacts on Si fabricated by rapid thermal annealing
J. Vac. Sci. Technol. B **17**, 397 (1999); 10.1116/1.590568

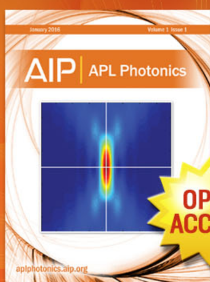

Launching in 2016!
The future of applied photonics research is here
AIP | APL Photonics

[This article is copyrighted as indicated in the article. Reuse of AIP content is subject to the terms at: http://scitation.aip.org/termsconditions. Downloaded to] IP: 103.21.127.60 On: Thu, 10 Sep 2015 10:41:17

JOURNAL OF APPLIED PHYSICS **116**, 124507 (2014)

Nano-scale NiSi and n-type silicon based Schottky barrier diode as a near infra-red detector for room temperature operation

S. Roy,[1,2] K. Midya,[3,2] S. P. Duttagupta,[3,2,a] and D. Ramakrishnan[4]
[1]*Centre for Nanotechnology and Science, Indian Institute of Technology Bombay, Mumbai 400076, India*
[2]*Centre of Excellence in Nanoelectronics, Indian Institute of Technology Bombay, Mumbai 400076, India*
[3]*Department of Electrical Engineering, Indian Institute of Technology Bombay, Mumbai 400076, India*
[4]*Department of Earth Science, Indian Institute of Technology Bombay, Mumbai 400076, India*

(Received 18 August 2014; accepted 12 September 2014; published online 24 September 2014)

The fabrication of nano-scale NiSi/n-Si Schottky barrier diode by rapid thermal annealing process is reported. The characterization of the nano-scale NiSi film was performed using Micro-Raman Spectroscopy and X-ray Photoelectron Spectroscopy (XPS). The thickness of the film (27 nm) has been measured by cross-sectional Secondary Electron Microscopy and XPS based depth profile method. Current–voltage (I–V) characteristics show an excellent rectification ratio ($I_{ON}/I_{OFF} = 10^5$) at a bias voltage of ± 1 V. The diode ideality factor is 1.28. The barrier height was also determined independently based on I–V (0.62 eV) and high frequency capacitance–voltage technique (0.76 eV), and the correlation between them has explained. The diode photo-response was measured in the range of 1.35–2.5 μm under different reverse bias conditions (0.0–1.0 V). The response is observed to increase with increasing reverse bias. From the photo-responsivity study, the zero bias barrier height was determined to be 0.54 eV. *© 2014 AIP Publishing LLC*. [http://dx.doi.org/10.1063/1.4896365]

I. INTRODUCTION

There have been a number of reports concerning the design, fabrication, and test of Near Infra-Red (NIR) detectors. The conventional photo-detector for 1.5 μm application is based on $In_xGa_{1-x}As$ hetero structures on InP or GaAs substrate.[1–4] The device fabrication is via Molecular Beam Epitaxy (MBE) or Metal Organic Chemical Vapour Deposition (MOCVD) process. With a few exceptions there is, in general, a lattice mismatch problem involving thick, multiple hetero-structure layers and the substrate which are required for efficient photo-response (8 A W^{-1} at 1.5 μm).[4] There exist specialized techniques such as buffered or lateral growth for reducing lattice mismatch, however this result in decreased throughput and increased cost.

Bandhyopadhyay *et al.* have demonstrated NIR detector based on photo responsive capacitance based on GaSb nano-wires.[5,6] As a result of tunability of capacitance, a shift in resonant peak frequency (in an LC circuit) is observed and accordingly a change in the power delivered to the load. The detectivity is reported to be 3×10^7 Jones. The process is potentially low cost and the device characteristics are observed to be reproducible and with a satisfactory shelf-life. However, this process is not silicon CMOS compatible. Further, the device testing scheme requires an in-built, high frequency, on-chip ac source (100 kHz and above) which adds to system complexity and cost.

Liu *et al.* have reported InAs nano-structures based on a cost-effective thermal CVD process. The nano-wires are subsequently suspended in anhydrous ethanol and transferred onto a silicon (or silicon dioxide) substrate. The responsivity was reported to be 4.4×10^3 A W^{-1} at 532 nm (visible region).[7] In contrast, Miao *et al.* have demonstrated InAs nano-wires grown by MBE process on GaAs substrate. The maximum responsivity in this case was reported to be 5.3×10^3 A W^{-1} in the visible region; however, photo-response was observed up until 1470 nm.[8]

Although the devices discussed above are quite efficient; however, the fabrication processes are mostly not CMOS compatible and cost-effective. Nevertheless, in opto-electronic devices silicon technology is considered inappropriate due to the indirect nature of the band gap. One way to resolve this drawback is to apply Silicide/Silicon Schottky Barrier Diodes (SBDs) for infra-red detection. The primary advantages of such diodes are a low (suitable for IR) and a tunable barrier height (depends on silicide type) formation. Of the possible silicide–silicon combinations, the PtSi/*p*-Si SBDs are widely used in the semiconductor industry. Due to the extensive application of PtSi SBDs in imaging technology, it has been widely used in Focal Plane Array.[9] The Schottky Barrier Height (SBH) of PtSi/*p*-Si has been reported in the range of 0.22–0.26 eV,[10–12] which corresponds to a cutoff wavelength of 4.77–5.64 μm. For lower cutoff wavelengths (8–10 μm)IrSi/*p*-Si SBDs had been proposed with a barrier height of 0.125–0.152 eV.[10,13] In contrast, for higher cutoff wavelengths ($\sim$3.7 μm), Pd_2Si SBD with SBH of $\sim$0.33 eV has been used.[14,15] Hence, such diodes are operable in the mid and far infrared regions.

This study aims at developing and optimizing SBDs for detection of NIR. For this purpose, nano-scale nickel silicide on *n*-Si diodes was fabricated. Previously, Zhu *et al.*[16] have demonstrated the utility of $NiSi_2$/*n*-Si SBDs for NIR (1.5 μm) region with a photo-responsivity of $\sim$2 mA/W. It was observed that the barrier height of nickel silicide (NiSi) n-Si SBDs is $\sim$0.66 eV;[17–20] hence, the cut off wavelength is $\sim$1.87 μm. Therefore, such diodes are suitable for optical communication application ($\lambda = 1.3$–1.5 μm)[21] and also for detection of hydrocarbon gases.[22] The Ni–Si phase diagram predicts six stable inter-metallic compound (Ni_3Si, $Ni_{31}Si_{12}$,

[a]Electronic mail: sdgupta@ee.iitb.ac.in

 © 2014 AIP Publishing LLC

[This article is copyrighted as indicated in the article. Reuse of AIP content is subject to the terms at: http://scitation.aip.org/termsconditions. Downloaded to] IP: 103.21.127.60 On: Thu, 10 Sep 2015 10:41:17

Ni_2Si, Ni_3Si_2, NiSi, and $NiSi_2$).[23] NiSi is considered to be the most promising candidate for electronic devices since it is stable with very low specific resistivity (of the order of 7–10 $\mu\Omega$-cm),[23] which should result in high photo-responsivity of nano-scale NiSi/*n*-Si SBDs.

In this paper, we have investigated performance of NiSi SBD. The diode was fabricated by deposition of Ni on Si followed by Rapid Thermal Annealing (RTA). The device has been characterized to investigate the optical response, and it is observed that the cutoff wavelength is around $\sim$2.3 μm. Hence, such devices opened up the possibility in the field of IR sensor in NIR region. The photo-responsivity of the developed diode is observed to be better than the earlier reported works.[16] However, improvements presumably results for the improvement of silicide-silicon interfaces.

II. EXPERIMENTAL DETAILS

The device has been fabricated using *n*-type Si (100) wafer of resistivity 1–10 Ω-cm. First of all, Radio Corporation of America cleaning was performed to remove native oxide and organic contaminants from the surface of the wafer. A 100 nm SiO_2layer was grown by wet oxidation process for contact pad deposition. Back side SiO_2 of the wafer was etched by Buffered Hydro Fluoric (BHF) acid after then n^+ region was made by ion implantation followed by 30 s RTA at 950 °C. A 0.5 $\times$ 1 mm^2 window was constructed by optical lithography process, and selective removal of SiO_2 was done from the surface by the BHF. Pattering for top electrode was performed on the SiO_2 window for Ni deposition. After patterning, wafer was dipped into BHF to remove native oxide formed during the process. Following the removal of native oxide, the wafer was immediately loaded in electron beam evaporator chamber for Ni deposition. Deposition was performed at a base vacuum of 5×10^{-6} mbars. A 10 nm Ni film was deposited on the patterned Si substrate followed by lift-off. Subsequently, RTA was performed at 500 °C for 60 s for silicide formation. The unreacted Ni was removed by treating with an acid mixture (HNO_3:HCl = 1:5 for 60 s). Finally, Au was deposited for top contact (1 $\times$ 1 mm^2) and Ti/Au was deposited for back ohmic contact.

The electrical characterization of diode was performed using Keithley 4200 instrument. Optical response was measured using Keithley 2400 under illumination of a tungsten lamp with a mono-chromator arrangement. Cross-sectional Secondary Electron Microscopy (SEM) (Raith-150) technique was used to investigate the thickness of the silicide. X-ray Photoelectron Spectroscopy (XPS) (PHI5000VersaProbe-II) and Raman spectroscopic measurement (RAMNORHG-2S) were performed to get material signature. The area of top silicide contact has been measured using microscope and was found to be 8.4×10^{-4} cm^2. The schematic diagram of cross-sectional view of the device is shown in Fig. 1.

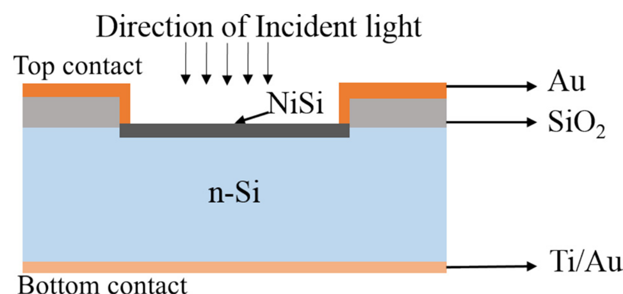

FIG. 1. Cross-sectional diagram of device.

III. RESULTS AND DISCUSSIONS

A. Materials characterizations

Raman spectroscopic analysis was performed to verify the phase composition of the silicide film (Fig. 2) using 514.5 nm argon ion laser (10 mW power) source. The intense peak observed at 522 cm^{-1} is attributed to silicon wafer. This Si peak is significant for our study, which indicates that all the compositional information of film has been gathered till the substrate. Another set of four peaks (shown in the inset of Fig. 2) at 199, 217, 294, and 363 cm^{-1} are attributed to the NiSi phase.[24,25] The peak at 217, 294, and 363 cm^{-1} are assigned to A_g mode whereas 199 cm^{-1} assigned to the B_{1g} mode.[26] A slight sift ($\sim$1 cm^{-1}) of peak compared to as reported by the Karabko *et al.*[26] has been observed. A small shoulder peak observed at 371 cm^{-1} is attributed to a formation of $NiSi_2$ phase in the film.[27]

Peak corrections of XPS spectrum were performed by carbon (C 1s) peak (at 284.5 eV) position. The spectrum of the film is shown in Fig. 3. The peak position at 853.9 eV and 871 eV of Ni2$p_{3/2}$ and Ni2$p_{1/2}$ (shown in the inset of Fig. 3(a), respectively, corresponds to NiSi phase.[23] Along with that a small overlapping peak of Ni2$p_{3/2}$ position has been observed at 854.6 eV which corresponds to $NiSi_2$ phase. From the low peak intensity at 854.6 eV, it is concluded that the fraction of $NiSi_2$ phase present in the film is less than NiSi phase. This validates the observation of Raman analysis shown in Fig. 2. The Si 2p spectrum is shown in Fig. 3(b). The peak position found at 99.4 eV also attributes to NiSi phase. It is verified from both XPS and Raman analysis as that NiSi phase has been formed along with a small fraction of $NiSi_2$.

Cross-sectional SEM imaging was performed to investigate the thickness of silicide film. The image is shown in Fig. 4 indicates that the NiSi film is uniform and the thickness has been found to be 27 nm (shown in the inset of Fig. 4).

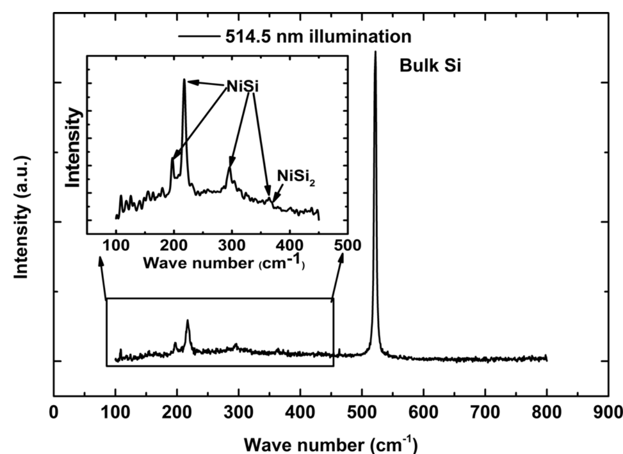

FIG. 2. Raman analysis spectrum silicide film by 514.5 nm Ar ion laser source.

[This article is copyrighted as indicated in the article. Reuse of AIP content is subject to the terms at: http://scitation.aip.org/termsconditions. Downloaded to] IP: 103.21.127.60 On: Thu, 10 Sep 2015 10:41:17

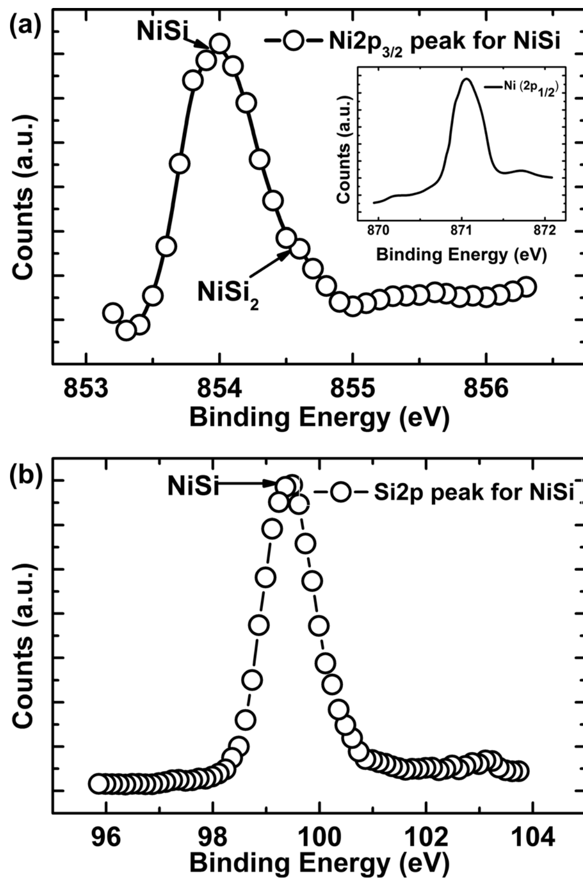

FIG. 3. (a) Ni 2p3/2 XPS spectrum for NiSi film. Inset shows Ni2p1/2 spectrum for NiSi film. (b) Si2p XPS spectrum of the film to investigate NISi phase.

The atomic concentration of Ni and Si in nickel-silicide was calculated by peak intensities using the following equation:

$$C_x = \frac{(I_x/S_x)}{\sum_i (I_i/S_i)}, \tag{1}$$

where C_x, I_x, and S_x are the atomic concentration, peak intensity, and sensitivity, respectively, of xth element. The sensitivity value is determined by the instrument manufacturer (Ni 2p3/2: 4.04 and Si 2p: 0.339). Argon plasma etching (etch rate of 2.4 nm/min) was performed to investigate the depth profile of film. The change in atomic fraction of Ni and Si with the variation of nano-film thickness is shown in Fig. 5.

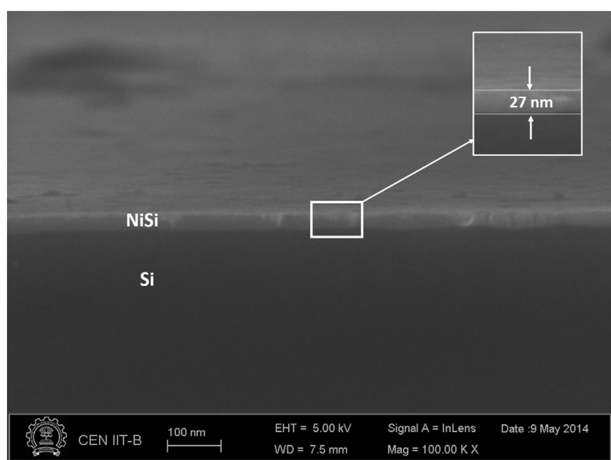

FIG. 4. Cross-sectional SEM image of NiSi/Si interface to investigate film thickness as well as the interface of the metal semiconductor junction.

It is observed from Fig. 5 that the ratio of Ni and Si is constant for approximately 27 nm. Then, the atomic fraction of Ni decreases to zero and Si fraction increases to 1. This indicates that NiSi phase formed and the composition is uniform till 27 nm. The variation of Ni and Si compositional ratio with depth is shown in the inset of Fig. 5. This observation correlates with the results obtained from SEM image. Since the volume fraction of $NiSi_2$ is much less in comparison to NiSi phase, $NiSi_2$ formation is considerable insignificant.

B. Electrical characterization

1. I-V characterization

The current–voltage (I–V) characteristics of NiSi/n-Si Schottky diode at different temperatures are shown in Fig. 6(a). The results indicate that the diode is Schottky in nature. The rectification ratio (I_{on}/I_{off}) has been observed to be $\sim 10^5$ at ± 1 V (at room temperature). The forward bias I–V relation of Schottky diode is expressed as[28–30]

$$I = I_0(\exp(e(V - IR_S)/nkT) - 1), \tag{2}$$

where

$$I_0 = A^* A T^2 \exp(\phi_B^{I-V}/kT). \tag{3}$$

I_0 is the reverse saturation current which has been calculated by I–V plot by considering I·R_s value is very small ($R_s \sim 50$ Ω for our device).

The electrical parameter of Schottky diode was extracted when $V > 3kT/e$. ln(I) vs V plot is shown in the inset of Fig. 6(b). The Richardson plot ($\ln(I_0/T^2)$ vs 1000/T) is shown in Fig. 6(b). Barrier height (ϕ_B^{I-V}) has been

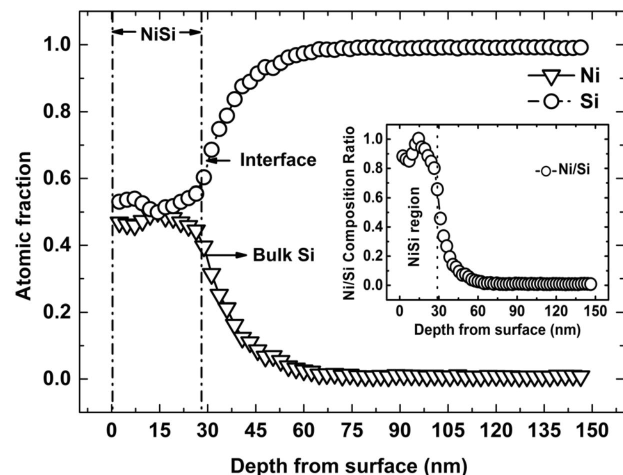

FIG. 5. Depth profile of NiSi film to investigate the atomic fraction of the film with the variation of depth. Inset shows the Ni and Si compositional ratio of the film with variation of depth.

[This article is copyrighted as indicated in the article. Reuse of AIP content is subject to the terms at: http://scitation.aip.org/termsconditions. Downloaded to] IP: 103.21.127.60 On: Thu, 10 Sep 2015 10:41:17

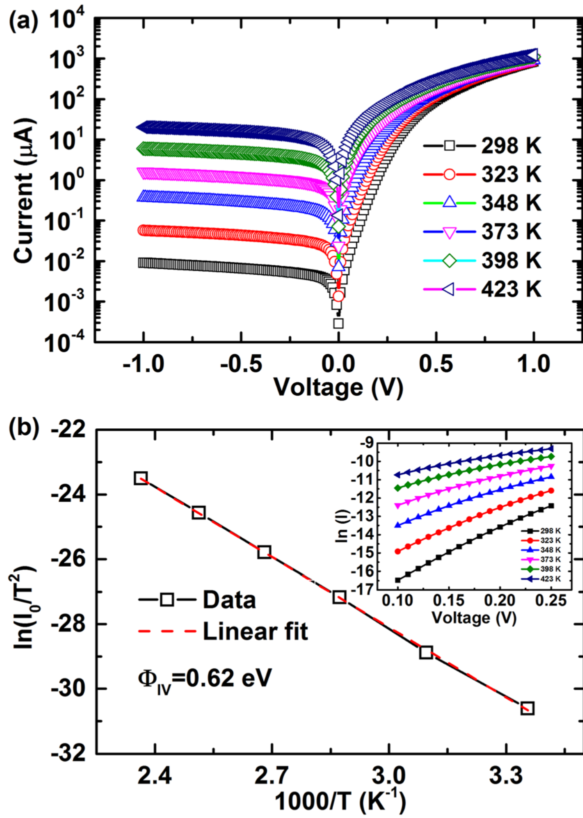

FIG. 6. (a) I-V characteristics of NiSi/n-Si SBD at different temperature. (b) Richardson plot of NiSi/n-Si diode to find out barrier height. Inset shows the ln(I) vs V to find out I_0 value.

calculated from the slope of Richardson plot and it is found to be 0.62 eV. The barrier height is comparable to as reported by Chang and Erskine.[18] The ideality factor (n) has been calculated at room temperature which is determined to be 1.28.

2. C–V characterization

Capacitance–voltage (C–V) measurement is another well-established technique to calculate barrier height (ϕ_B^{C-V}) of the Schottky diode. The $1/C^2$ vs V characteristic of NiSi/n-Si Schottky diode in the reverse bias voltage (0 V–1 V) at a frequency of 1 MHz is shown in Fig. 7. The Schottky Mott

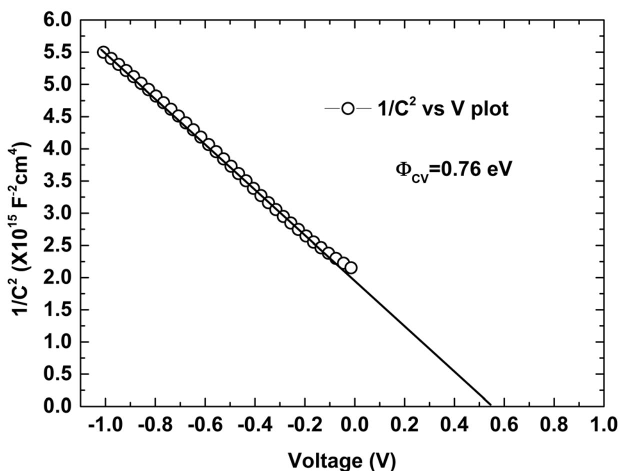

FIG. 7. $1/C^2$ vs V plot of NiSi/n-Si Schottky diode measured at 1 MHz.

model and abrupt junction approximation are implemented to determine the carrier concentration (N_d). N_d has been calculated by following equations:[28,31]

$$\frac{1}{C} = \sqrt{\frac{2(V_{bi}-V)}{2N_d e\varepsilon_s}}, \tag{4}$$

$$N_d = \frac{2}{e\varepsilon_s}\left[\frac{1}{d(1/C^2)/dV}\right]. \tag{5}$$

ϕ_B^{C-V} has been calculated by calculating the intercept (V_{bi}) of $1/C^2 (=0)$ at voltage axis, and using the following equation:[28,29]

$$\phi_B^{C-V} = V_{bi} + V_n + \frac{kT}{e}, \tag{6}$$

$$V_n = \frac{kT}{e}\ln\left(\frac{N_c}{N_d}\right). \tag{7}$$

The value of N_d has been derived and it is found to be $5\times10^{15}\,\mathrm{cm}^{-3}$. Accordingly, ϕ_B^{C-V} value is found 0.76 eV.

For low doped ($\sim10^{15}\,\mathrm{cm}^{-3}$) substrate where tunnelling current is not significant, the relation between the ϕ_B^{C-V} and ϕ_B^{I-V} has been proposed by Broom *et al.*[32] The relation is expressed as

$$\phi_{Bcal}^{I-V} = \frac{\phi_B^{C-V} + V_n(n-1)}{n}, \tag{8}$$

where ϕ_{Bcal}^{I-V} is calculated value of zero bias barrier height (ϕ_B^{I-V}) and it has been found to be 0.64 eV which closely matches to ϕ_B^{I-V} (0.62 eV).

C. Optical measurement

The photo-responsivity (R) of NiSi/*n*-Si SBD, with wavelength (λ) under different reverse bias, is shown in Fig. 8(a). The value of R is found to be increasing with decrease illumination wavelength. Similar characteristics are observed for different bias conditions. It is observed from Fig. 8(b) that the responsivity is promising (2.6 mA/W for zero bias condition at 1.5 μm). The photo-responsivity of the SBDs is approximated by Fowler equation, expressed as[33,34]

$$R = C_1\left(1 - \frac{\phi_B^{opt}}{h\nu}\right)^2, \tag{9}$$

where C_1 is the constant, ϕ_B^{opt} is barrier height of SBD, and $h\nu$ is the energy of incident photon. The characteristic of photo-responsivity at zero bias is shown in Fig. 8(b). Fowler plot ($h\nu\sqrt{R}$ vs $h\nu$) was made for zero bias condition to calculate the zero bias barrier height (inset of Fig. 8(b)). ϕ_B^{opt} was calculated at the intersection of extrapolation of $h\nu\sqrt{R}$ to the $h\nu$ axis, and the value has been found to be 0.54 eV. The barrier height value observed in this case is much less than that derived by I–V and $1/C^2$–V method. Such behaviour attributed to presence of acceptor like trap state at the interface.[35]

With the incidence of photons on the silicide, the valence band electrons at interface region are excited and trapped by acceptor like trap state. Hence, those trap states becomes

[This article is copyrighted as indicated in the article. Reuse of AIP content is subject to the terms at: http://scitation.aip.org/termsconditions. Downloaded to] IP: 103.21.127.60 On: Thu, 10 Sep 2015 10:41:17

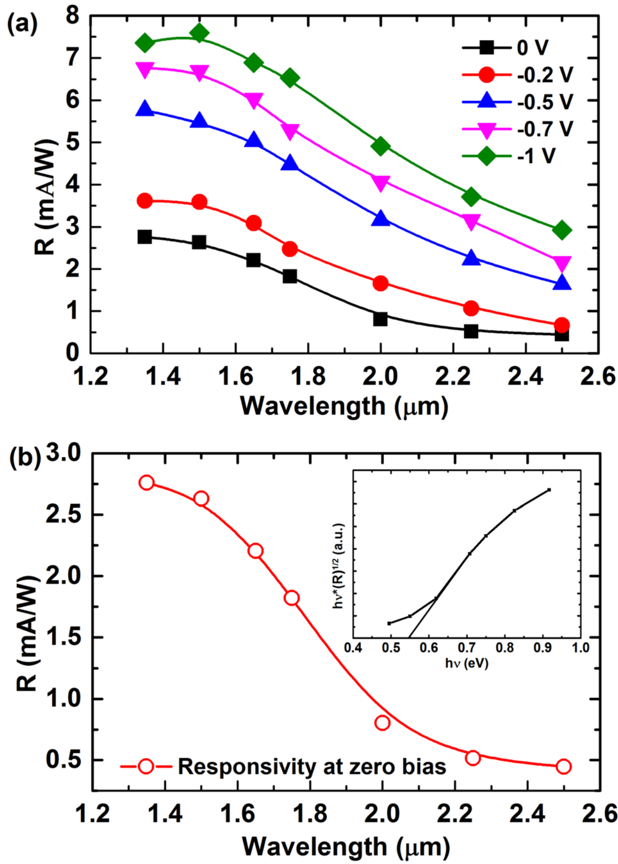

FIG. 8. (a) Photo-response of NiSi/n-Si Schottky diode measured at different reverse bias condition. (b) Photo-response of NiSi/n-Si Schottky diode measured at zero bias condition. Inset shows the Fowler plot to find out zero bias barrier height.

negatively charged. These negatively charge states contribute to the Fermi energy band. In other word, the Fermi level shifting towards the conduction band occurs, which effectively reduces the band bending and hence, the barrier height reduction of the SBD occurs. The estimated electrical parameters at room temperature are listed in Table I.

The variation of photo-responsivity with reverse bias at different irradiation wavelength is shown in Fig. 9. It is observed that the photo-responsivity increases monotonically with increase in reverse bias, and the diode response for 1.35 and 1.5 μm has been found to be similar.

The relation between photo current (photo-responsivity) to the bias voltage for Metal-Semiconductor-Metal (MSM) diode has been proposed by Nejad *et al.*[36] which can be expressed as

$$R = R_o \exp\left(-\frac{B}{V}\right), \tag{10}$$

where R_o and B are constants, which depends on the irradiating photon energy. The plot of ln(R) vs 1/V plot (shown in inset of Fig. 9), the linearity of the plot indicates that the photo-response with bias voltage of this device obey the relation expressed in Eq. (10).

TABLE I. Table of electrical parameters of NiSi/n-Si Schottky diode.

n	ϕ_B^{I-V} (eV)	ϕ_B^{C-V} (eV)	ϕ_{Bcal}^{I-V} (eV)	ϕ_B^{opt} (eV)
1.28	0.62	0.76	0.64	0.54

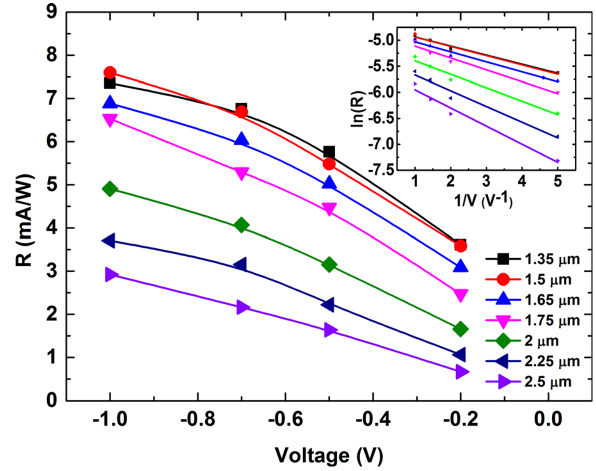

FIG. 9. Responsivity vs reverse bias of NiSi/n-Si Schottky diode at different illumination photon energy.

IV. CONCLUSION

This study demonstrates fabrication of a nano-scale NiSi/n-Si Schottky infrared detector SBD, fabricated by RTA process with top bottom contacts. The formation of NiSi phase has been confirmed by Raman and depth sensitive XPS technique. The silicide film thickness has been measured by SEM, which is found to be 27 nm and verified by XPS technique. The barrier height has been measured by I–V, C–V, and optical process. The barrier height obtained from I–V is closely matched with reported values, whereas that evaluated from optical process differs. The variations of barrier height have been explained by the presence of acceptor like interface trap states. Such trap states capture the photo–exited the electrons form valence band which further contribute to the Fermi energy level. Therefore, it eventually lowers the band bending and reduces the barrier height. The device photo-responsivity has been observed and found to be promising comparable to the reported values. The responsivity was measured at different reverse bias conditions and it has been found that the response follows the relation as proposed by the earlier works for MSM diode. The responsivity can be enhanced by improving the interface and creating an optical cavity. Hence, it can be concluded that this diode has extensive potential application in the field of gas detection by IR absorption method and optical communication.

ACKNOWLEDGMENTS

We would like to express thanks to Mr. H. Singh Bana, Department of Electrical Engineering, Indian Institute of Technology Bombay for his assistance in chemical process and V. K. Bajpai, Department of Energy Science, Indian Institute of Technology Bombay for cross-sectional SEM imaging.

[1]J. Kaniewski and J. Piotrowski, Opto-Electron. Rev. **12**, 139 (2004).
[2]A. Rogalski, Opto-Electron. Rev. **20**, 279 (2012).
[3]Y. Zhang, Y. Gu, C. Zhu, G. Hao, A. Li, and T. Liu, Infrared Phys. Technol. **47**, 257 (2006).

[This article is copyrighted as indicated in the article. Reuse of AIP content is subject to the terms at: http://scitation.aip.org/termsconditions. Downloaded to] IP: 103.21.127.60 On: Thu, 10 Sep 2015 10:41:17

[4]J. Kaniewski and J. Piotrowski, Opto-Electron. Rev. **5**, 225 (1997).
[5]S. Bandhyopadhyay, J. Appl. Phys. **116**, 023108 (2014).
[6]S. Bandhyopadhyay and J. Anderson, Appl. Phys. Lett. **102**, 103108 (2013).
[7]Z. Liu, T. Luo, B. Liang, G. Chen, G. Yu, X. Xie, D. Chen, and G. Shen, Nano Res. **6**, 775 (2013).
[8]J. Miao, W. Hu, N. Guo, Z. Lu, L. Liao, S. Shi, P. Chen, Z. C. Ho, T.-X. Li, X. S. Chen, and W. Lu, ACS Nano **8**, 3628 (2014).
[9]W. F. Konosocky, F. V. Shallcross, T. S. Villani, and J. V. Groppe, IEEE Trans. Electron Devices **32**, 1564 (1985).
[10]B. Y. Tsaur, M. M. Weeks, and P. W. Pellegrni, IEEE Electron Device Lett. **9**, 100 (1998).
[11]V. W. L. Chin, J. W. V. Storey, and M. A. Green, J. Appl. Phys. **68**, 4127 (1990).
[12]J. B. Bindell, E. F. Labuda, and W. M. Moller, IEEE Trans. Electron Devices **27**, 420 (1980).
[13]S. Petersson, J. Baglin, W. Hammer, F. D'Heurle, T. S. Kuan, I. Ohdomari, J. de Sousa Pires, and P. Tove, J. Appl. Phys. **50**, 3357 (1979).
[14]S. Chand and J. Kumar, Semicond. Sci. Technol. **10**,1680 (1995).
[15]W. Cabanski and M. Schulz, Infrared Phys. **32**, 29 (1991).
[16]S. Zhu, M. B. Yu, G. Q. Lo, and D. L. Kwong, Appl. Phys. Lett. **92**, 081103 (2008).
[17]S. Thomas and L. E. Terry, J. Vac. Sci. Technol. **13**, 156 (1976).
[18]Y.-J. Chang and J. L. Erskine, Phys. Rev. B **28**, 5766 (1983).
[19]Q. T. Zhao, U. Breuer, E. Rije, St. Lenk, and S. Mantl, Appl. Phys. Lett. **86**, 062108 (2005).
[20]A. Xia, F. C. Hui, H. Ru, G. Yue, H. Cong, Z. Xing, and W. Y. Yuan, Chin. Phys. B **18**, 4465 (2009).
[21]M. C. Bost and J. E. Mahen, J. Appl. Phys. **58**, 2696 (1985).
[22]G. Farca, S. I. Shopova, and A. T. Rosenberger, Opt. Express **15**, 17443 (2007).
[23]Y. Cao, L. Nyborg, and U. Jelvestam, Surf. Interface Anal. **41**, 471 (2009).
[24]P. S. Lee, D. Mangelinck, K. L. Pey, Z. X. Shen, J. Ding, T. Osipowicz, and A. See, Electrochem. Solid-State Lett. **3**, 153 (2000).
[25]S. K. Donthu, D. Z. Chi, S. Tripathy, A. Wong, and S. J. Chua, Appl. Phys. A **79**, 637 (2004).
[26]A. O. Karabko, A. P. Dostanko, J. F. Kong, and W. Z. Shen, J. Appl. Phys. **105**, 033518 (2009).
[27]W. S. Lee, T.-H. Chen, C.-F. Lin, and J.-M. Chen, Mater. Trans. **52**, 1374 (2011).
[28]D. A. Neamen, *Semiconductor Physics and Devices* (Tata McGraw Hill, New York, 2007), p. 318.
[29]S. M. Sze, *Physics of Semiconductor Devices*, 2nd ed. (Wiley-Interscience, New York, 1981).
[30]U. Kunze and W. Kowalsky, J. Appl. Phys. **63**, 1597 (1988).
[31]E. Rhoderick and R. William, *Metal Semiconductor Contacts* (Oxford Clarendon, 1988), p. 51.
[32]R. F. Broom, H. P. Meier, and W. Walter, J. Appl. Phys. **60**, 1832 (1986).
[33]J. Cohen, R. J. Archer, and J. Vilms, *Investigation of Semiconductor Schottky Barriers for Optical Detection and Cathodic Emission* (Defense Technical Information Center, 1968).
[34]W. K. Kosonocky, "Review of Schottky barrier imager technology," Proc. SPIE **1308**, 2 (1990).
[35]B. K. Li, C. Wang, I. K. Sou, W. K. Ge, and J. N. Wang, Appl. Phys. Lett. **91**, 172104 (2007).
[36]S. M. Nejad, S. E. Maklavani, and E. Rahimi, in *Dark Current Reduction in ZnO-Based MSM Photodetector with Interfacial Thin oxide Layer: Proceedings of the International Symposium on High Capacity Optical Networks and Enabling Technologies* (IEEE, Penang, Malaysia, 2008), p. 259.

[This article is copyrighted as indicated in the article. Reuse of AIP content is subject to the terms at: http://scitation.aip.org/termsconditions. Downloaded to] IP: 103.21.127.60 On: Thu, 10 Sep 2015 10:41:17